KAPOK-CHITOSAN-ECH COMPOSITE BEADS AS AN EFFICIENT AND SUSTAINABLE ADSORBENT FOR REACTIVE BLACK 5 DYE REMOVAL FROM AQUEOUS SOLUTION

JIN-YING TONG,[*] SIEW-TENG ONG[*,**] and SIE-TIONG HA[*,**]

[*]*Department of Chemical Science, Faculty of Science, Universiti Tunku Abdul Rahman, Jalan Universiti, Bandar Barat, 31900 Kampar, Perak, Malaysia*
[**]*Centre for Agriculture and Food Research, Universiti Tunku Abdul Rahman, Jalan Universiti, Bandar Barat, 31900 Kampar, Perak, Malaysia*
✉ *Corresponding author: S.-T. Ong, ongst@utar.edu.my; ongst_utar@yahoo.com*

Received July 4, 2026

From waste to functionalized adsorbent, agricultural by-products are being redefined as efficient materials for wastewater treatment applications. This study investigated the removal of Reactive Black 5 (RB5) dye from aqueous solution using Kapok husks-chitosan-epichlorohydrin (KH-CH-ECH) composite beads. Comprehensive characterization of KH-CH-ECH composite beads was conducted using attenuated total reflectance-Fourier transform infrared spectroscopy to determine the surface functional groups, whereas scanning electron microscopy and atomic force microscopy to provide detailed insights into surface morphology and three-dimensional topography, respectively. Energy-dispersive X-ray spectroscopy and X-ray diffraction analysis were further conducted for elemental analysis, and evaluation of the crystallinity and structural characteristics of the KH–CH–ECH composite beads, respectively. The adsorption performance was evaluated through batch experiments, in which the key factors, such as contact time, initial RB5 concentration, adsorbent dosage, agitation rate and pH were included. It was found that the kinetics of RB5 sorption fitted a pseudo-second order rate expression. Freundlich isotherm model with R^2 value of 0.9992 was found to best fit the equilibrium data. Maximum adsorption capacity obtained from this study was determined to be 33.8983 mg/g. Plackett–Burman design was first employed to screen significant factors, which were subsequently optimized using Response Surface Methodology. Optimization results revealed that maximum uptake removal of RB5 (100%) occurred at optimum conditions of 212.5 minutes contact time, 0.125 g of KH-CH-ECH composite beads and at pH 3.

Keywords: Kapok husks, chitosan, epichlorohydrin, Reactive Black 5, composite beads

INTRODUCTION

Water pollution and agricultural waste accumulation are often regarded as two independent environmental challenges. However, what if one problem could be utilized to address the other? As industrialization continues to expand worldwide, increasing volumes of wastewater containing pollutants are discharged into aquatic environments. At the same time, large quantities of agricultural residues are generated annually and discarded or underutilized despite their potential value. Transforming agricultural waste into functional materials for wastewater treatment offers a strategy that simultaneously addresses both environmental concerns, while promoting sustainable resource utilization.

Among the various industrial pollutants, synthetic dyes are of particular concern because of their extensive use in textile, paper, leather and dye-manufacturing industries. They are well known for their stability and excellent colour fastness. It is estimated that 15% of the dyes used during manufacturing processes ultimately enters wastewater streams, resulting in highly colored effluents that are difficult to be treated.[1,2] The presence of dyes not only deteriorates quality of water bodies, but also reduces light penetration, disrupts photosynthetic activity, decreases dissolved oxygen levels and adversely affects aquatic ecosystems.[3-5] Furthermore, many synthetic dyes are toxic, mutagenic and carcinogenic, and their high chemical stability and

resistance to biodegradation allow them to persist in the environment for prolonged periods, posing serious risks to both environmental and human health.[6,7]

Among the various classes of dyes, reactive dyes are particularly problematic because of their high water solubility and complex molecular structures, which hinder their removal by conventional treatment processes. RB5, one of the most widely used reactive azo dyes, is widely used in the textile industry due to its strong affinity towards textile fibers.[8] However, RB5 contains azo (-N=N-) linkages and aromatic structures that contribute to its persistence in aquatic environments. [9,10] Furthermore, the degradation of azo dyes may produce potentially toxic aromatic amines, contribute to long-term environmental pollution. Beyond its environmental persistence, RB5 poses potential risks to both human health and aquatic life. Previous studies have reported that long-term exposure of RB5 has been linked to various adverse effects, including skin irritation, respiratory disorders and carcinogenic risks, whereas even trace concentrations can impart intense coloration to water bodies.[11,12]

Various treatment technologies, including coagulation-flocculation, membrane filtration, advanced oxidation processes, chemical precipitation and biological treatment, have been employed for dye removal. Although these methods can be effective under certain conditions, they often suffer from drawbacks such as high operational costs, sludge generation or membrane fouling.[13] In comparison, adsorption has emerged as one of the most attractive treatment approaches due to its simplicity, high efficiency, ease of operation and ability to remove dyes without generating harmful by-products.[14,15] The effectiveness of adsorption, however, largely depends on the characteristics and cost of the adsorbent employed. In recent years, increasing attention has been directed towards the utilization of agricultural residues as low-cost and sustainable adsorbents.[16-19] Such materials are renewable, widely available and often contain abundant compounds with functional groups capable of interacting with dye molecules.

Among the vast array of agricultural residues generated worldwide, *Ceiba pentandra* (L.) Gaertn. remains one of the most overlooked biomass resources. Derived from the fruit of *Ceiba pentandra* (L.) Gaertn., a tropical tree that widely distributed throughout Southeast Asia, Kapok is primarily valued for its lightweight cotton-like fibers and seed-derived oil.[20] The value of Kapok has been defined by what lies inside it for decades. In contrast, the husk, which is the structure that protects these valuable components, has received remarkably little attention and is commonly discarded as waste after harvesting. This perception, therefore, may overlook a material with considerable environmental potential. This is because Kapok husks are rich in lignocellulosic compounds and surface functional groups capable of interacting with pollutant molecules.[21,22] Hence, rather than viewing Kapok husk as a disposal burden, it may be more appropriately regarded as a naturally occurring platform for adsorption.

On the other hand, chitosan, a value-added biopolymer derived from chitin-rich waste, such as shrimp and crab shells, has gained attention as a promising adsorbent due to its presence of reactive amino and hydroxyl functional groups. However, its structural weakness in aqueous solution often limits its practical performance.[23] In this context, ECH acts as effective crosslinking agent by reacting primarily with hydroxyl group of chitosan, while preserving and exposing the accessibility of amino sites.[24,25]

To the best of our knowledge, no study has been available so far in the literature to combine Kapok husks and chitosan to synthesize KH-CH-ECH composite beads. Hence, in this work, a novel KH-CH-ECH composite material was developed and investigated as adsorbent for RB5 removal from aqueous solutions.

EXPERIMENTAL

Chemicals

Chitosan from crab shell (flakes) with 80% degree of acetylation was purchased from Nacalai Tesque. Epichlorohydrin, acetic acid and sodium hydroxide pellets were purchased from Sigma Aldrich and Merck, respectively. All the chemicals were used as received.

Preparation of Kapok husk powder

Collected Kapok was initially processed by separating the husk from the attached fibers. The separated husks were subsequently cut into smaller pieces before being thoroughly washed with tap water, followed by rinsing with distilled water to ensure the removal of any dirt and impurities. After the cleaning process, the samples were oven-dried at 60 °C for 24 hours to remove residual moisture. Once dried, a grinder was used to grind the dried KH into powder form and screened through a series of sieves to obtain uniform particle sizes. KH powder with the sizes

ranging from 106 to 250 μm were selected for further use in this study.

Preparation of Kapok husks-chitosan-epichlorohydrin composite beads

CH solution was prepared by dissolving 3 g of CH flakes in 2% v/v acetic acid solution and continuously stirred for 24 hours to obtain a homogeneous CH solution. KH powder (6 g) was added in towards the end of the stirring process to obtain a mixture of KH-CH solution. This mixture was then added dropwise into 0.5 M of sodium hydroxide (NaOH) bath to form the KH-CH composite beads. The beads obtained were then filtered and the washing process was repeated until it achieved a neutral pH. After washing, the wet beads were immersed in 0.5% v/v ECH solution at 40 °C for two hours for the crosslinking reaction. The crosslinked beads were washed again with distilled water to remove excess ECH solution. Finally, the beads were subjected to drying and the obtained beads were labelled as KH-CH-ECH composite beads.

Preparation of adsorbate

Reactive Black 5 with the molecular formula of $C_{26}H_{21}N_5Na_4O_{19}S_6$ and CI No. 20505 was chosen as the adsorbate. RB5, with a dye content of more than 50% was obtained from Sigma Aldrich and used without any purification. Standard dye solutions of 1000 mg/L were prepared as stock solutions and subsequently diluted when necessary.

Characterization studies

XRD patterns of the samples were recorded on an X-ray Diffractometer (Shimadzu XRD 6000) operated at a voltage of 40 kV and current of 30 mA with Cu Kα characteristic radiation. The scanning range was carried out from 10° to 90° 2θ.

Attenuated Total Reflectance-Fourier Transform Infrared (ATR-FTIR) spectroscopy was performed using Perkin Elmer Spectrum 2 FT-IR spectrometer. ATR-FTIR analysis was employed to determine the presence of surface functional group on the KH-CH-ECH composite beads. The KH-CH-ECH composite beads were analyzed both before and after the adsorption of RB5 in the wavenumber range of 400-4000 cm^{-1}. The surface morphology of KH-CH-ECH composite beads before and after adsorption of RB5 was studied using a Scanning Electron Microscope (SEM) equipped with energy dispersive X-ray Spectrometer (SEM-EDX) JEOL-JSM 6701 F SEM. A Park XE-70 Atomic Force Microscope (AFM) was used to analyze the surface topography of KH-CH-ECH composite beads before and after the adsorption of RB5. The samples were scanned in non-contact mode over a scan area of 1 × 1 μm^2.

Batch studies

The adsorption experiments were carried out in centrifuge tubes by agitating the composite beads with 20 mL of RB5 solution on an orbital shaker. The supernatant was withdrawn at specific time intervals and its final dye concentration was analyzed using a UV-Vis spectrophotometer at the wavelength of 598 nm, corresponding to its maximum absorption wavelength. To ensure the reliability of the results, all the batch experiments were conducted in duplicates and the mean values were used for data analysis. Simultaneously, a control experiment in the absence of KH-CH-ECH composite beads was included to ascertain that the observed sorption does not depend on the walls of the centrifuge tubes, but resulted solely from the composite beads.

To study the effect of initial RB5 concentration on the adsorption performance, RB5 solutions with initial concentrations of 25, 50 and 75 mg/L were prepared. In each experiment, 0.20 g of KH-CH-ECH composite beads were introduced into different concentration of RB5 solutions and shaken at 150 rpm. Samples were collected at different time intervals (5, 10, 15, 30, 60, 120, 180, 240, 300, 360, 420 and 480 minutes) for UV–Vis analysis.

The effect of adsorbent dosage on the uptake of RB5 was investigated by adding 0.05, 0.10, 0.15, 0.20 and 0.25 g of KH-CH-ECH composite beads into 20 mL of 25 mg/L RB5 solution for three hours to attain equilibrium.

For the effect of agitation rate, experiments were performed at agitation rates of 50, 150 and 200 rpm, while maintaining other experimental conditions constant.

In the study on the effect of pH, a series of pH ranging from pH 3 to 11 of the 25 mg/L RB5 solution were prepared. For each run, a fixed amount of KH-CH-ECH composite beads (0.20 g) was introduced into the RB5 solution on the orbital shaker with 150 rpm agitation rate for three hours. The different pH of the RB5 solutions were adjusted using dropwise addition of 0.01, 0.05, 0.10 and 1.0 M of HCl and NaOH solutions.

Sorption isotherms were obtained by varying the RB5 concentration from 20 to 60 mg/L. In each experiment, the RB5 solution was in contact with 0.10 g of KH-CH-ECH composite beads until equilibrium was attained at ambient temperature.

Using the pH drift method, the point of zero charge (pH_{pzc}) was obtained by measuring the initial pH of RB5 solutions containing the KH-CH-ECH composite beads and the final pH after 24 hours. The initial pH ranged from pH 2 to 12. pH_{pzc} can be obtained from the plot of ΔpH versus initial pH where ΔpH equals to zero.

Plackett-Burman design

Plackett–Burman (PB) design was used to screen and identify the factors that significantly influence RB5 adsorption. The design assessed the main effects of factors at two levels (high and low). Factors tested included contact time, initial dye concentration,

adsorbent dosage, agitation rate and pH. Twelve experimental runs were carried out following the design matrix produced by statistical software, with each run performed under its assigned conditions.

Optimization of uptake removal of RB5 using Response Surface Methodology

Response Surface Methodology (RSM) was used to optimize the adsorption process conditions and to evaluate the interactive effects between significant factors identified from the screening study. Experiments were carried out according to the CCD matrix generated by statistical software and the response, defined as the uptake removal of RB5, was measured under each set of conditions. All experimental design and statistical evaluations were carried out using Design Expert Version 7.1.3.

RESULTS AND DISCUSSION

Characterization studies

XRD

The XRD pattern of the KH–CH–ECH composite beads (Fig. 1) exhibited a broad diffraction feature centred at approximately 2θ = 20-22°, accompanied by a shoulder around 15–17°. These diffraction regions are commonly associated with the ordered polysaccharide domains of cellulose and chitosan.[26-28] However, the broad peak profile indicated the predominance of amorphous regions within the composite. KH-CH-ECH composite beads was determined to have a degree of crystallinity of 9.58% and an amorphous content of 90.42%, indicating that the material is predominantly amorphous with only a small fraction of ordered crystalline domains. Such characteristic was expected for lignocellulosic-chitosan composites, as the coexistence of cellulose and chitosan alongside highly amorphous hemicelluloses and lignin resulted in a predominantly amorphous structure.[29]

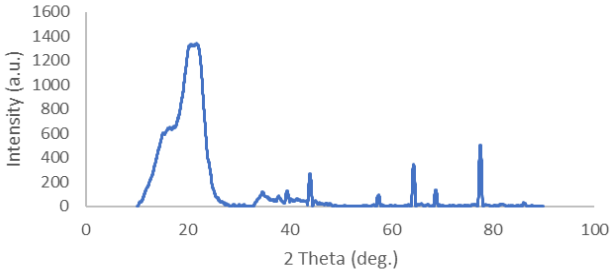


Figure 1: XRD pattern of KH-CH-ECH composite beads

ATR-FTIR

Figure 2 shows the ATR-FTIR spectra of the KH-CH ECH composite beads before and after RB5 adsorption. Kapok husks are mainly composed of lignocellulosic compounds, including cellulose, hemicelluloses and lignin, whereas chitosan is a naturally occurring polysaccharide derived from chitin. The bands observed at 3472 and 3417 cm^{-1} were corresponding to the overlapping of O-H and N-H stretching vibrations of the hydroxyl groups in the lignocellulosic components and the amino groups of chitosan, respectively.[21,30] The peaks located at 2925 and 2851 cm^{-1} were attributed to the asymmetric and symmetric stretching vibrations of aliphatic C-H bonds, respectively.[31-33] The absorption band at 1638 and 1619 cm^{-1} was assigned to the NH bending and amide I band of chitosan, corresponding to the C=O stretching vibration of the $NHCOCH_3$ group, while contributions from the conjugated carbonyl (C=O) groups of lignin present in Kapok husk may also overlap within this region.[34-36] In addition, the absorption peak located at 1510 cm^{-1} was associated with the aromatic ring skeletal (C=C) stretching vibrations of lignin, which is one of the principal structural constituents of Kapok husk.[37] Furthermore, the band appearing at 1379 cm^{-1} can be related to amide III C-N stretching vibrations of chitosan together with C-H bending vibrations associated with lignocellulosic components.[38,39] The asymmetric stretching of C-O-C linkage present in polysaccharide structures was observed at 1155 cm^{-1}, whereas the bands located at 1069 cm^{-1} was associated with C-O stretching vibrations originating from chitosan, cellulose, hemicellulose and lignin.[40-43] A characteristic band at 893 cm^{-1} was an indicative of β-(1→4)-glycosidic linkages.[44]

Following the adsorption of RB5, only minor variations were observed in the spectrum. This behaviour was expected, as adsorption predominantly occurs through surface interactions rather than major change to the chemical structure

of the adsorbent.[45] Nevertheless, several characteristic bands exhibited shifting accompanied by variations in peak intensity following RB5 adsorption (Table 1). The overlapping of O-H and N-H stretching region showed a pronounced difference after adsorption, indicating that these functional groups may have contributed to the interaction with RB5 molecules during dye uptake. Additionally, two new absorption bands appeared at 1334 and 1229 cm^{-1}, which correspond closely to the characteristic wavenumbers reported for RB5, further supported the successful adsorption of RB5 onto the composite beads.[46]

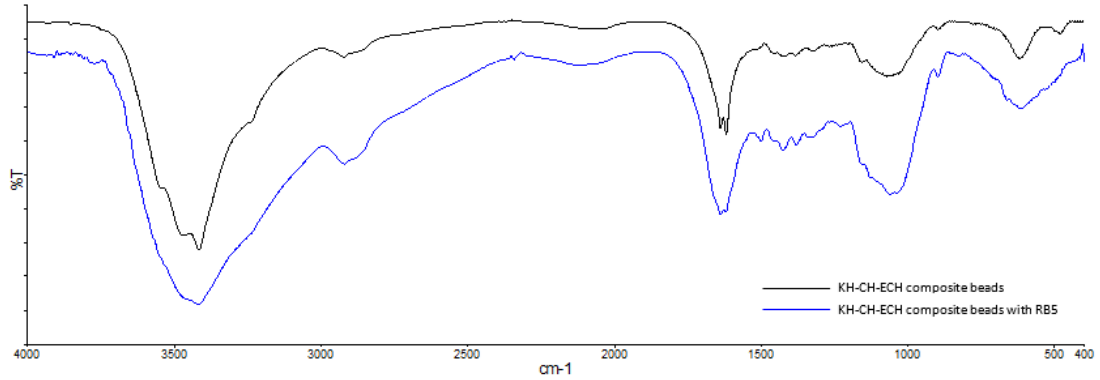


Figure 2: ATR-FTIR spectra of KH-CH-ECH composite beads before and after the adsorption of RB5

Table 1
Comparison of IR absorption peaks before and after adsorption of RB5

Wavenumber (cm^{-1})		Assignment
Before adsorption	After adsorption	
3472, 3417	3466, 3417	OH and NH stretching
2925	2921	Asymmetric CH stretching
2851	2874	Symmetric CH stretching
1510	1501	C=C aromatic ring stretching
1379	1376	C-N stretching, CH bending
-	1334, 1229	Characteristic vibrations of RB5 functional groups
1069	1060	C-O stretching

SEM

The surface morphology of the KH-CH-ECH composite beads before and after the adsorption of RB5 was examined using SEM and the corresponding micrographs are presented in Figure 3. As shown in Figure 3(a), KH-CH-ECH composite beads exhibited a relatively compact and smooth surface with the absence of pores and limited surface irregularities. Such morphology reflected the native structure of the composite beads before interaction with RB5 dye molecules.

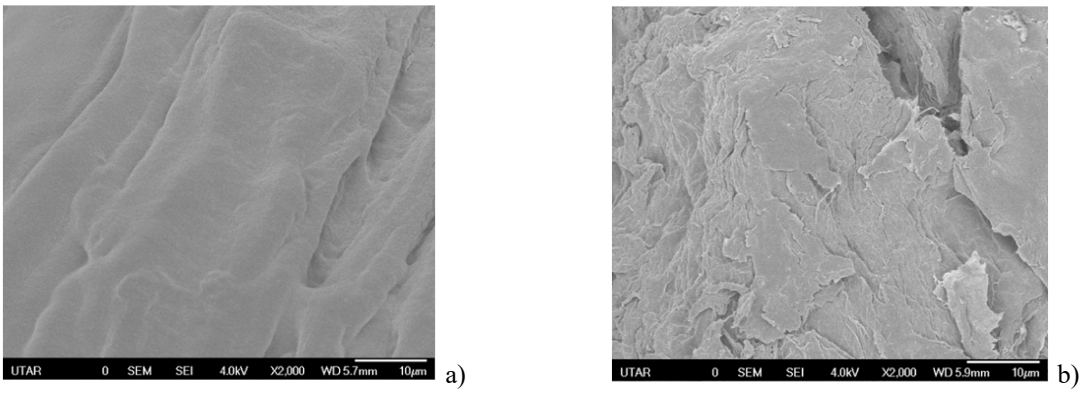
After the adsorption of RB5 (Fig. 3(b)), a transformation in surface characteristics was observed. The previously smooth surface became significantly roughened and structurally heterogeneous, accompanied by the appearance of irregular folds, flake-like formations and layered textures. In addition, the presence of surface deposits and irregular protrusions suggested the accumulation of RB5 molecules on the surface of KH-CH-ECH composite beads. These deposited species likely formed a layer that altered the original surface texture of the composite beads. The morphological differences observed after adsorption therefore confirmed the successful uptake of RB5.

EDX

EDX analysis was conducted to investigate the elemental composition of the KH-CH-ECH composite beads before and after the adsorption of RB5 and the results are presented in Figure 4. Prior to adsorption, the EDX spectrum revealed the presence of only carbon (C) and oxygen (O), which are the predominant elements associated with the lignocellulosic constituents of Kapok husk and the polysaccharide structure of chitosan.

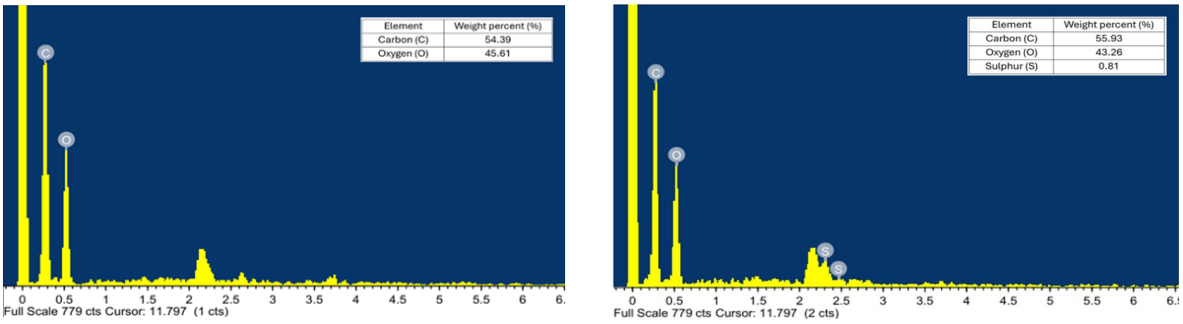
After the adsorption of RB5, the EDX spectrum continued to exhibit carbon and oxygen signals, indicating that the fundamental elemental

composition of the composite beads remained mainly unchanged. Interestingly, a new signal corresponding to sulphur (S) was detected after adsorption, with a sulphur content of 0.81 wt%. The appearance of sulphur was particularly significant because sulphur was absent before adsorption and this was believed to be originated from the sulphonate ($-SO_3^-$) groups present in the molecular structure of RB5.[47] Hence, the detection of sulphur after the adsorption of RB5 further confirmed the successful attachment of RB5 molecules onto the surface of the KH-CH-ECH composite beads.



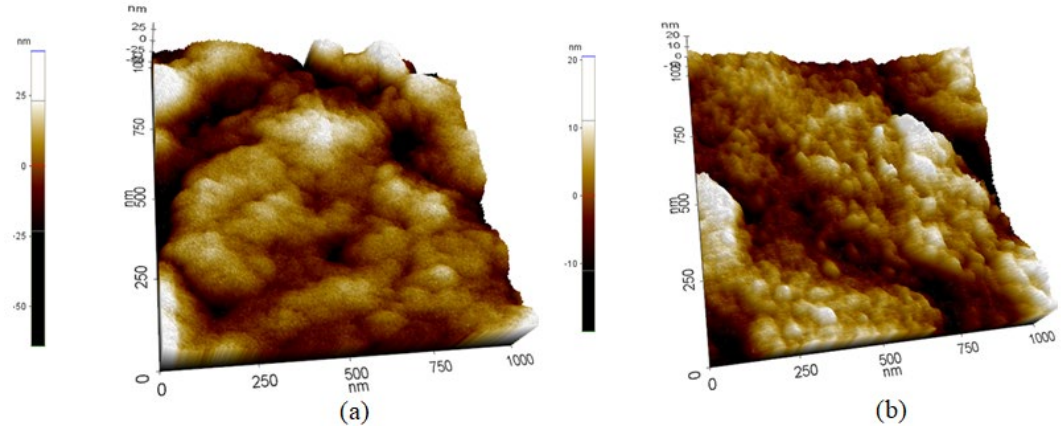
a) b)

Figure 3: SEM micrographs of KH-CH-ECH composite beads (a) before and (b) after the adsorption of RB5



(a) (b)

Figure 4: EDX spectra of KH-CH-ECH composite beads (a) before and (b) after the adsorption of RB5



(a) (b)

Figure 5: AFM micrographs of KH-CH-ECH composite beads (a) before and (b) after the adsorption of RB5

AFM

AFM analysis was performed to investigate the surface topography of the KH-CH-ECH composite beads before and after adsorption of RB5 at the nanometer scale. As shown in Figure 5(a), the surface of the KH-CH-ECH composite beads exhibited a rough and an irregular topography with the presence of darker region distributed across the scanned area. Darker region means lower topography and lighter region means

higher topography. Such surface features provide potential adsorption sites that facilitate the interaction between the adsorbent and dye molecules.

After adsorption, brighter and more elevated regions became more prominent, accompanied by the appearance of agglomerated and granular features distributed across the scanned area. It was believed to be the deposition and accumulation of RB5 molecules on the surface of KH-CH-ECH composite beads. In addition, the average surface roughness (R_a) of the composite beads decreased from 9.012 to 4.541 nm after adsorption of RB5, indicating a substantial reduction in surface irregularity. This decrease in roughness can be attributed to the adsorption of RB5 molecules on the adsorbent surface, which partially filled the dent area and covered the exposed surface features. Hence, these observations further supported the adsorption findings.

Batch studies

Effect of contact time and initial RB5 concentration

The adsorption profiles obtained at different initial RB5 concentrations exhibited a similar characteristic two-stage behaviour (Fig. 6). A pronounced increase in RB5 dye removal was observed during the early stages of adsorption, followed by a gradual approach towards equilibrium. It can be observed that the adsorption was rapid in the first 30 minutes for all the three initial concentrations of RB5. This trend suggested that the adsorption process was initially governed by external mass transfer, where RB5 molecules were rapidly transported across the boundary layer from the bulk solution to occupy the readily accessible large amount of adsorption sites on the surface of KH-CH-ECH composite beads during the initial stage.[48,49]

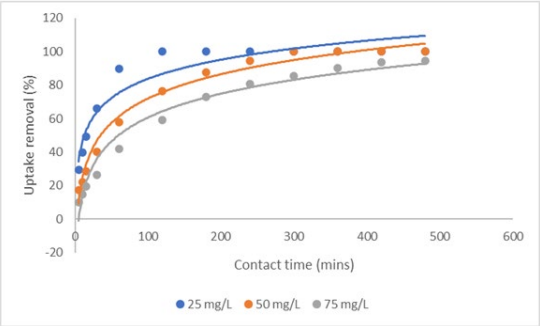


Figure 6: Effect of contact time and initial RB5 concentration on adsorption performance



Figure 7: RB5 solutions at different contact times, and KH-CH-ECH composite beads after adsorption

Over time, the rate of adsorption gradually decreased as more and more surface adsorption sites of KH-CH-ECH composite beads became occupied. With fewer surface sites remaining, intraparticle diffusion became increasingly important, whereby RB5 molecules had to diffuse into the internal structure to access the less accessible regions of the beads. Since intraparticle diffusion is generally slower than the external mass transfer, the overall adsorption rate decreased until equilibrium was attained.[50,51] Based on Figure 6, the equilibrium time was found to be dependent on the initial RB5 concentration. At 25 mg/L RB5, equilibrium was reached rapidly within 120 minutes, whereas longer contact times were required for higher concentrations, with 50 and 75 mg/L reaching equilibrium at 300 and 420 minutes, respectively. This may be due to the greater number of RB5

molecules that needed to be adsorbed before the adsorption sites became saturated.

The visual appearance of the RB5 solution at different contact times is presented in Figure 7. An evident gradual decolorization from a dark blue-black solution to complete decolorization was observed with increasing adsorption time, proving the effective uptake of RB5 by the KH–CH–ECH composite beads.

Effect of adsorbent dosage

The effect of dosage of KH-CH-ECH composite beads on the uptake of RB5 was shown in Figure 8. From Figure 8, it can be clearly seen that the system followed the usual trend whereby the uptake removal increased as the dosage of composite beads increased.[15,52] The influence of dosage of KH-CH-ECH composite beads on the removal efficiency of RB5 was primarily dependent on the availability of active binding sites and overall surface area of the adsorbent.

When 0.05 g of KH-CH-ECH composite beads was added, the obtained uptake of RB5 in three hours was only 56.30%. This is because at lower dosages, the number of available active sites on the composite beads was insufficient to effectively interact with all RB5 molecules in the solution, thus leading to lower removal efficiency. When higher mass of KH-CH-ECH composite beads was used, it provided greater availability of active adsorption sites and increased surface area on the composite beads, which then enhances the probability of the interactions between RB5 molecules and KH-CH-ECH composite beads. In this adsorption system, saturation occurred at 0.20 g of KH-CH-ECH composite beads, at which further increases in the dosage had negligible influence on adsorption performance. The plateau behaviour was attributed to the attachment of all RB5 molecules on the surface of the composite beads and RB5 molecules now became the limiting factor.[53,54] Hence, the increase in removal efficiency became less pronounced at higher dosages as saturation and equilibrium has been reached.

Effect of agitation rate

According to Figure 9, the results showed that agitation rate played a role in controlling both uptake rate and removal efficiency. When 50 rpm of agitation rate was used, it can be observed that the adsorption process proceeded at a slower rate and a noticeably lower RB5 removal was observed in the beginning of the process. It was only able to achieve 42.22% in the first 30 minutes, which is much lower than for the other agitation rates. This indicated that insufficient contact led to more pronounced external mass transfer resistance. In contrast, increasing the agitation rate to 150 rpm markedly improved the adsorption performance, resulting in substantially higher removal and a much faster approach to equilibrium as compared to 50 rpm. This is because higher agitation enhanced the diffusion of dye molecules to the surface of the adsorbent by decreasing the boundary layer thickness and improving mass transfer efficiency.[55-57] However, a further increase to 200 rpm brought only a slight improvement and the adsorption profile overlapped with that at 150 rpm, with equilibrium being reached only slightly earlier.

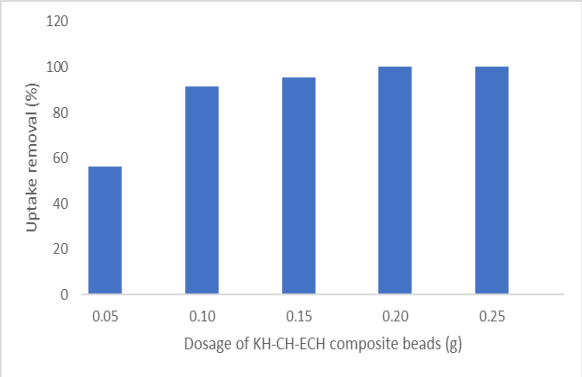


Figure 8: Effect of dosage of KH-CH-ECH composite beads on RB5 uptake removal

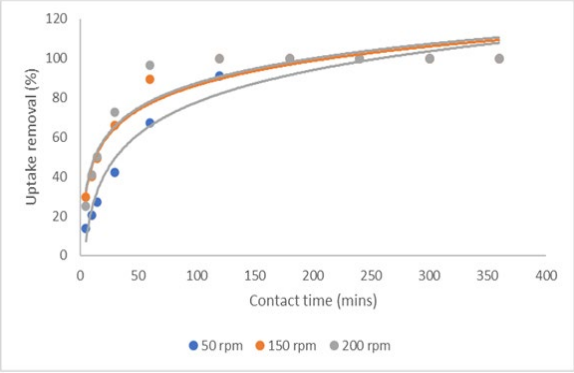


Figure 9: Effect of different agitation rates on the removal of RB5 by KH-CH-ECH composite beads

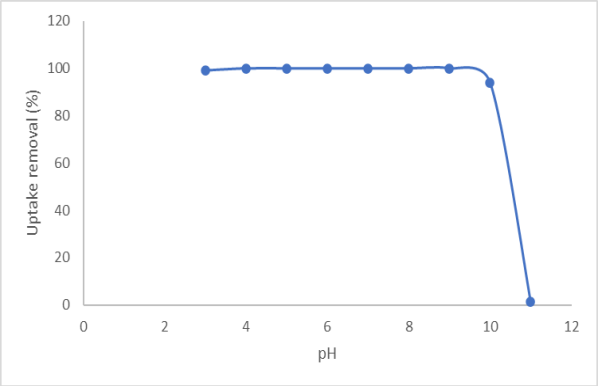


Figure 10: Effect of pH on the adsorption of RB5 by using KH-CH-ECH composite beads

This can be attributed to the fact that beyond 150 rpm, external film diffusion resistance becomes minimal until the system approaches a region where agitation no longer plays a dominant role in affecting the adsorption.[57,58]

Hence, the results indicated that sufficient agitation is necessary to reduce boundary layer resistance, while excessively high agitation beyond the optimum level offers minor benefits for the system. Consequently, 150 rpm was chosen as the optimum agitation rate in this adsorption system.

Effect of pH

The adsorption process can be strongly influenced by solution pH, as pH can alter the surface characteristics of the adsorbent, the dissociation behavior of functional groups at active sites and the degree of ionization of both the adsorbent and the adsorbate.

Based on Figure 10, it can be seen that the removal of RB5 remained constantly high under acidic to near neutral conditions. In the pH range of 3 to 9, the uptake was relatively stable and maintained at approximately 98 to 100%. This indicated that the surface of the KH-CH-ECH composite beads remained sufficiently favourable for RB5 adsorption across this pH range. The adsorption of RB5 was not studied under extremely acidic and basic conditions (pH 2 and pH 12) as a decrease in absorbance value and shifting in the lambda max of the control solution was observed when the RB5 solution was adjusted to these pH values. A slight decrease in removal efficiency was observed at pH 10, followed by a sharp drop at pH 11, where the uptake was only 1.35%.

As RB5 is an anionic dye, its adsorption is generally due to electrostatic interactions with the surface of the composite beads, which are dependent on the pH_{pzc} of the KH-CH-ECH composite beads.[59] The pH_{pzc} of the KH-CH-ECH composite beads was determined to be pH 6.54. Hence, at low pH and nearly neutral pH conditions, the functional groups on the surface of the composite beads undergo protonation resulting in a positively charged surface. This would contribute to the electrostatic attraction between the positively charged surface of KH-CH-ECH composite beads and negatively charged sulfonate group ($–SO_3^-$) present on RB5 molecules.[60,61] Conversely, when the pH increased to slightly basic conditions, the uptake of RB5 decreased slightly. The abrupt reduction of uptake at strongly basic conditions was attributed to the increased electrostatic repulsion between the negatively charged surface of the composite beads and the anionic RB5 molecules.[62] From the current results, an appreciable amount of dye can still be removed at pH values above pH_{pzc} and this is most probably due to the involvement of other sorption interactions, such as van der Waals forces, π-π interactions and hydrogen bonding occurring at the same time.[53] Additionally, the competition with excess hydroxyl ions for active binding sites may have further weakened the interactions between RB5 molecules and KH-CH-ECH composite beads.[8,60]

Adsorption isotherms

Langmuir isotherm

The Langmuir isotherm model is described as:[63]

$$q_e = \frac{q_m K_L C_e}{1 + K_L C_e} \quad (1)$$

The constant, q_m and K_L can be determined from the linearized form of Equation (1) and the linear form is:

$$\frac{C_e}{q_e} = \frac{1}{q_m K_L} + \frac{C_e}{q_m} \quad (2)$$

where C_e = RB5 concentration at equilibrium (mg/L), q_e = amount of RB5 adsorbed at equilibrium (mg/g), q_m = maximum adsorption capacity of KH-CH-ECH composite beads for RB5 removal (mg/g), K_L = Langmuir isotherm constant related to energy of KH-CH-ECH composite beads (L/mg).

A plot of C_e/q_e versus C_e yielded a straight line of slope $1/q_m$ and an intercept of $1/q_mK_L$. The Langmuir model adequately described the adsorption equilibrium data, yielding a coefficient of determination (R^2) of 0.9912 (Fig. 11). Based on this model, the calculated maximum adsorption capacity of KH-CH-ECH composite beads, q_m and Langmuir isotherm constant, K_L were 33.8983 mg/g and 0.05277 L/mg, respectively. In addition, the favorability of the adsorption process was assessed using the dimensionless separation factor (R_L), which resulted in a range from 0.2400 to 0.4865. Since the R_L values fell between 0 and 1, the adsorption of RB5 onto the KH-CH-ECH composite beads is considered favorable.

Langmuir model allows the calculation of maximum adsorption capacity, which is useful for the comparison of the adsorption efficiency of different materials. The q_m value obtained in this study was relatively higher than those reported for several adsorbents in previous studies.[11,58,64-66] The results suggested that KH-CH-ECH composite beads are capable of binding RB5 molecules effectively and demonstrated their potential to serve as a competitive alternative to other low-cost adsorbents in dye removal applications.

Freundlich isotherm

The Freundlich isotherm model is defined as an exponential equation:[67]

$$q_e = K_F C_e^{\frac{1}{n}} \quad (3)$$

The linearized equation is expressed as:

$$\log q_e = \frac{\log C_e}{n} + \log K_F \quad (4)$$

where q_e = amount of RB5 adsorbed at equilibrium (mg/g), C_e = concentration of RB5 at equilibrium (mg/L), n = Freundlich constant for intensity, K_F = Freundlich isotherm constant for adsorption capacity.

A plot of log q_e against log C_e was constructed. According to Figure 12, the Freundlich plot exhibited an excellent fit to the experimental data, with R^2 value of 0.9992. The Freundlich constants, K_F and n, which represent the adsorption capacity and adsorption intensity, respectively, were found to be 1.8993 and 1.2107, respectively. The n value of 1.2107, which is more than one, again indicated a favourable adsorption of RB5 onto the KH-CH-ECH composite beads and reflected the high affinity of the adsorbent toward the RB5 dye molecules.

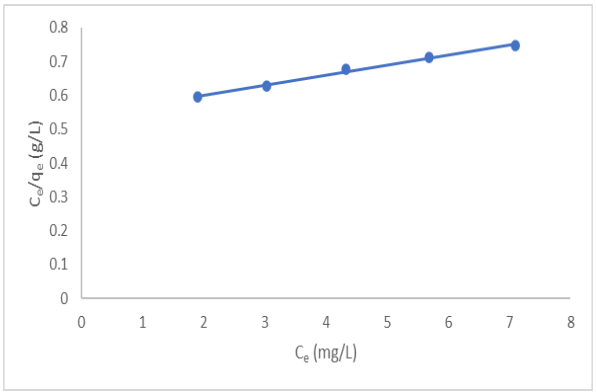


Figure 11: Langmuir isotherm plot for the removal of RB5 by KH-CH-ECH composite beads

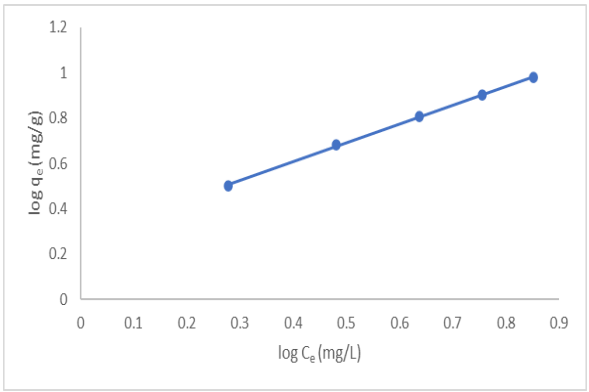


Figure 12: Freundlich isotherm plot for the removal of RB5 by KH-CH-ECH composite beads

Brunauer-Emmett-Teller (BET) isotherm

BET isotherm model is defined as:[68]

$$q_e = \frac{K_B q_m C_e}{(C_S - C_e)[1+(K_B-1)\left(\frac{C_e}{C_S}\right)]} \quad (5)$$

The equation can be linearized as follows:

$$\frac{C_e}{(C_S - C_e)q_e} = \left(\frac{K_B - 1}{K_B q_m}\right)\left(\frac{C_e}{C_S}\right) + \frac{1}{K_B q_m} \quad (6)$$

where q_e = amount of RB5 adsorbed at equilibrium (mg/g), K_B = BET constant, which describes the energy involved in the adsorbate-adsorbent interaction, q_m = amount of RB5 in formation of complete monolayer (mg/g), C_e =

concentration of RB5 at equilibrium (mg/L), C_s = RB5 concentration at saturation (mg/L).

The q_m and K_B were determined to be 33.8982 mg/g and 242161, respectively. The q_m obtained from this isotherm model matched well with the q_m values based on the Langmuir plot. A good linearity was observed over the studied concentration range (Fig. 13) and the high R^2 value of 0.9912 suggested that the adsorption of the RB5 molecules may be extended beyond monolayer coverage.

According to Table 2, all three isotherm models exhibited high R^2 values, indicating that each model provides a good description of the adsorption behaviour of the system. This suggested that the adsorption process may not be governed by a single ideal mechanism, but rather involves a combination of surface interactions. However, among the three models, the Freundlich isotherm still showed the highest R^2 value (very close to unity) and therefore, it is suggested that the interaction between RB5 and KH-CH-ECH composite beads can be best described by Freundlich isotherm model.

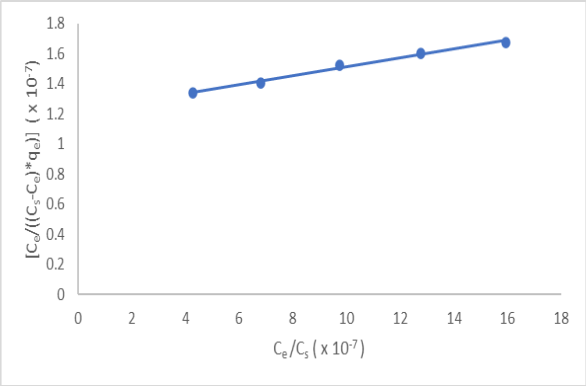


Figure 13: BET isotherm plot for the removal of RB5 by KH-CH-ECH composite beads

Table 2
Isotherms parameters and R^2 values of removal of RB5 by KH-CH-ECH composite beads

Langmuir isotherm		Freundlich isotherm		BET isotherm	
q_m (mg/g)	33.8983	n	1.2107	q_m(mg/g)	33.8982
K_L (L/mg)	0.0528	K_F	1.8993	K_B	242161
R^2	0.9912	R^2	0.9992	R^2	0.9912

Adsorption kinetics

Pseudo-first order kinetic model

Generally, the pseudo-first order kinetic model assumes that the rate of adsorption is proportional to the number of unoccupied adsorption sites. This model is often used to describe adsorption processes dominated by physical adsorption mechanisms.[69]

The linear form of the pseudo-first order kinetic model is the following:

$$\log(q_e - q_t) = \log q_e - \frac{k_1}{2.303} t \quad (7)$$

where q_e = amount of RB5 adsorbed at equilibrium (mg/g), q_t = amount of RB5 adsorbed at time t (mg/g), k_1 = pseudo-first order kinetics rate constant (min^{-1}), t = time (minutes).

Pseudo-second order kinetic model

In contrast, the pseudo-second order kinetic model assumes that the adsorption rate is controlled by the availability of adsorption sites and is often associated with chemisorption. The model further assumes that the rate of adsorption is proportional to the square of the number of unoccupied sites.[70]

The final pseudo-second order equation after integration is:

$$\frac{t}{q_t} = \frac{1}{h} + \frac{t}{q_e} \quad (8)$$

$$h = k_2 q_e^2 \quad (9)$$

where q_t = amount of RB5 adsorbed at time t (mg/g), k_2 = pseudo-second order kinetics rate constant (g/mg min), q_e = amount of RB5 adsorbed at equilibrium (mg/g), h = initial adsorption rate (mg/g min).

The kinetic data were analyzed using both pseudo-first and pseudo-second order kinetic models and the corresponding parameters are presented in Table 3. By comparing the R^2 values from both kinetic models, the results revealed that the pseudo-second order model provided a better description of the experimental data. The R^2 obtained from the pseudo-second order kinetic model ranged from 0.9929 to 0.9989, and were consistently higher than those obtained from the pseudo-first order kinetic model (0.9565–0.9940). It can be observed that the pseudo-second order rate constant (k_2) decreased with increasing initial RB5 concentration, indicating a slower adsorption rate at higher dye loadings. In addition, the equilibrium adsorption capacities calculated from the pseudo-second order kinetic model showed closer agreement with the experimental values. The above findings indicated that the pseudo-second order kinetic model more accurately described the adsorption behaviour of RB5 onto the KH-CH-ECH composite beads.

The excellent fit of the pseudo-second order model suggested that the rate limiting step may be chemisorption, which involved electron sharing or electron exchange between RB5 molecules and the functional groups present on the adsorbent surface. This finding is also consistent with the ATR-FTIR results whereby after the adsorption of RB5, an increase in band intensity was observed and this can be associated with stronger hydrogen bonding. Apart from that, a good uptake over a wide range of pH also supported the occurrence of different simultaneous interactions in the adsorption process. Similar adsorption behaviour has been widely reported for dye adsorption systems, where the pseudo-second order model is frequently found to be providing better fitting quality of the adsorption kinetics.[23,71-74]

The values of q_e, k_2 and h obtained from the pseudo-second order kinetic model were analyzed as a function of the initial RB5 concentration and regression equations were developed to describe their variation with C_o. The theoretical model derived for RB5 sorption by KH-CH-ECH composite beads is presented as:

$$q_t = \frac{C_o t}{(12.322)(C_o)+(-209.95)+(0.0191\ C_o+9.2836)t} \quad (10)$$

Based on Figure 14, it is clear that the theoretically generated curves agreed well with the experimental data for RB5 removal. The pseudo-second order rate law could provide a good prediction for the amounts of RB5 adsorbed. The theoretical adsorption capacity was in close agreement with the experimental, particularly at 25 mg/L RB5. With a higher RB5 concentration, this corresponds to an increase in competition for fixed adsorption sites and the growing influence of intraparticle diffusion and mass transfer resistance.

Table 3
Comparison of all parameters between pseudo-first and pseudo-second order kinetic models

Initial RB5 concentration (mg/L)	Pseudo-first order			Pseudo-second order				$q_{e,exp}$ (mg/g)
	$q_{e,cal}$ (mg/g)	k_1 (min^{-1})	R^2	$q_{e,cal}$ (mg/g)	k_2 (x 10^{-3} g/mg min)	h (mg/g·min)	R^2	
25	3.4562	0.0567	0.9623	2.5860	36.9870	0.2473	0.9989	2.5557
50	4.4208	0.0124	0.9940	5.4615	4.3848	0.1308	0.9975	4.9696
75	7.0162	0.0092	0.9565	7.9239	1.6117	0.1012	0.9929	6.8740

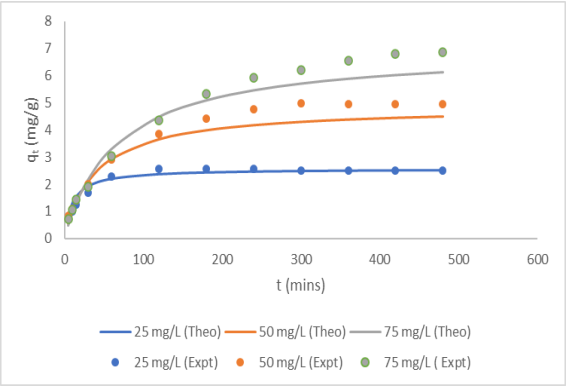


Figure 14: Comparison between theoretical and experimental adsorption capacity (pseudo-second order)

Therefore, a slight deviation from the assumption of pseudo-second order kinetic model was observed. Nevertheless, the overall agreement remained satisfactory, further supporting the suitability of the pseudo-second order kinetic model in describing the adsorption kinetics of RB5. It is proposed that ECH functions as a crosslinking agent through its reaction with hydroxyl groups of CH. This crosslinking may then enhance the accessibility of free amine ($–NH_2$) groups of CH, which serve as the primary active sites for the adsorption of RB5.

Plackett-Burman design

A total of five factors (contact time, initial RB5 concentration, adsorbent dosage, agitation rate and pH) were studied in PB and the ANOVA results were shown in Table 4. The results revealed that all investigated factors exhibited varying degrees of influence on the adsorption performance. The significant factors were identified based on their statistical significance ($p < 0.05$). Thus, among the five factors, contact time, adsorbent dosage and pH were identified as the significant factors as they had *p*-value of less than 0.05. These factors were found to have a strong impact on the removal efficiency of RB5. The significant factors selected from this screening stage were subsequently considered for further optimization using RSM, ensuring a more focused and efficient experimental design in the next stage of the study.

Table 4
Regression analysis (ANOVA) of Plackett-Burman for the adsorption of RB5

Source	Sum of squares	Degree of freedom	Mean square	F Value	*p*-value Prob > F
Model	14344.46	5	2868.89	25.79	0.0005
Contact time	8047.87	1	8047.87	72.35	0.0001
Initial RB5 concentration	120.47	1	120.47	1.08	0.3381
Adsorbent dosage	2192.28	1	2192.28	19.71	0.0044
Agitation rate	65.45	1	65.45	0.59	0.4721
pH	3918.39	1	3918.39	35.23	0.0010
Residual	667.37	6	111.23		
R-squared		0.9555	C.V.%		26.07
Adjusted R-squared		0.9185	Adequate precision		14.79
Predicted R-squared		0.8222			

Table 5
PB experimental conditions for RB5 removal by KH-CH-ECH composite beads, including the corresponding experimental and predicted uptake values

Experimental run	Factors					Experimental % uptake	Predicted % uptake
	Contact time (min)	Initial RB5 conc. (mg/L)	Adsorbent dosage (g)	Agitation rate (rpm)	pH		
1	5	25	0.05	50	3	8.75	13.60
2	5	25	0.05	200	3	17.70	18.27
3	5	25	0.20	50	10	7.73	4.49
4	5	75	0.05	200	10	2.95	3.38
5	5	75	0.20	200	3	43.13	49.41
6	5	75	0.20	50	10	7.05	10.83
7	420	25	0.05	50	10	23.62	29.26
8	420	25	0.20	200	3	100.00	97.10
9	420	25	0.20	200	10	65.88	65.10
10	420	75	0.05	50	3	81.53	71.73
11	420	75	0.05	200	10	27.04	40.26
12	420	75	0.20	50	3	100.00	98.77

Verification of Plackett-Burman design model

Model validation was carried out using the desirability function, whereby experiments were conducted under the optimal conditions proposed by the software. The findings in Table 5 showed good consistency between the predicted and experimental results. The differences between the predicted and experimental uptake removal were all below 13.2%. This confirmed the adequacy and reliability of the developed model.

Optimization of uptake removal of RB5 using Response Surface Methodology

RSM was employed to optimize the adsorption conditions of RB5 onto KH-CH-ECH composite beads and to evaluate the interaction effects between the significant factors. In this study, fifteen sets of experimental runs with different experimental conditions were generated by the software. After running each set of experimental runs, a quadratic model was developed to describe the relationship between the uptake of RB5 and the independent variables, including contact time, adsorbent dosage and pH.

The modified cubic model equation is as follows (11):

$$ln\,(Uptake\ removal) = 2.7450953 + 0.011288421(A) + 8.86437457(B) - 0.101234871(C) - 0.007973282(AB) + 0.00044537(AC) + 1.533815476(BC) - (1.92\,x\,10^{-5})(A^2) - 37.5965655(B^2) - 0.031605791(C^2)$$

where A = contact time, B = adsorbent dosage and C = pH.

The adequacy of the developed model was evaluated by ANOVA. Based on Table 6, the model F-value (65.94) indicated that the regression model was statistically significant. Meanwhile, all three factors studied had a *p*-value lower than 0.05, hence this further confirmed that the selected factors had a significant effect on the adsorption process. In this adsorption system, the model exhibited a high R^2 value of 0.9900, indicating that 99.00% of the variation in the response could be explained by the developed model. This demonstrated an excellent agreement between the experimental and predicted values. Furthermore, the adjusted R^2 value of 0.9750 was in reasonable agreement with the predicted R^2 value of 0.8807, with a difference of less than 0.1, suggesting good predictive capability and confirming that the model was not overfitted. Generally, a lower coefficient of variation (C.V.) reflects higher reliability of the experimental results and model predictions. In this study, the C.V. was found to be 6.10%, indicating good precision and reproducibility of the experimental data. In addition, the adequacy precision value of 29.621, which is considerably higher than the minimum desirable value of 4, indicated an adequate signal-to-noise ratio. Hence, this suggested that the model can effectively navigate the design space and can be used to predict the adsorption response with high confidence.

3D response surface plots were used to visualize the interaction effects between variables. These plots revealed that the adsorption efficiency was significantly influenced by the combined effects of factors rather than individual factors alone. In particular, interactions between contact time, adsorbent dosage and pH showed pronounced effects on RB5 removal efficiency. Figure 15(a) shows the 3D surface plot of the interaction between contact time and adsorbent dosage onto the removal of RB5. It was observed that the uptake increased with increasing contact time and adsorbent dosage, as evidenced by the transition from the blue region to the red region on the surface plot. At shorter contact times and lower dosages, the uptake was limited because fewer adsorption sites were available and the contact between RB5 and KH-CH-ECH composite beads was insufficient. As the contact time increased, more dye molecules had the opportunity to diffuse and interact with the active sites on the surface of the KH-CH-ECH composite beads, resulting in enhanced adsorption. Similarly, increasing the adsorbent dosage provided a greater number of available adsorption sites, thereby improving the uptake removal. However, beyond a certain dosage and contact time, it can be observed that the plot began to level off, suggesting that the adsorption approached equilibrium and that further increases in these variables will result in only minor improvements in dye removal.

Figure 15(b) presents the interactive effects of contact time and pH towards RB5 removal. The observed relationship between the uptake and contact time was in good agreement with the trend depicted in Figure 15(a), further confirming the positive effect of prolonged contact time on RB5 adsorption. In addition, higher removal was observed under acidic to near-neutral conditions, while a gradual decrease in removal efficiency occurred as the pH increased. This behaviour can be attributed to the protonation of amino groups on CH, which generated positively charged sites ($-NH_3^+$) that promote electrostatic attraction with the negatively charged RB5 molecules.

The relationship between adsorbent dosage and pH is shown in Figure 15(c). Similarly, the percentage uptake increased with dosage before reaching a plateau at higher dosages, following a pattern comparable to that illustrated in Figure 15(a), indicating a consistent influence of adsorbent dosage on the adsorption process. At lower pH values, the adsorption performance was substantially higher across the investigated dosage range. As the pH increased, a decline in uptake removal was observed despite the increase in adsorbent dosage.

Table 6
ANOVA of RSM for the adsorption of RB5 by KH-CH-ECH composite beads

Source	Sum of squares	Degree of freedom	Mean square	F Value	*p*-value Prob > F
Model	28.0604	9	3.1178	65.9388	< 0.0001
A-Contact time	10.8792	1	10.8792	230.0836	< 0.0001
B-Adsorbent dosage	3.3704	1	3.3704	71.2810	0.0002
C-pH	6.2425	1	6.2425	132.0233	< 0.0001
AB	0.1232	1	0.1232	2.6050	0.1577
AC	0.8370	1	0.8370	17.7008	0.0056
BC	1.2969	1	1.2969	27.4274	0.0019
A^2	1.8017	1	1.8017	38.1039	0.0008
B^2	0.1179	1	0.1179	2.4937	0.1654
C^2	0.3952	1	0.3952	8.3580	0.0277
Residual	0.2837	6	0.0473		
Lack of fit	0.2837	5	0.0567		
R-Squared		0.9900	C.V.%		6.10
Adjusted R-squared		0.9750	Adequate precision		29.62
Predicted R-squared		0.8807			

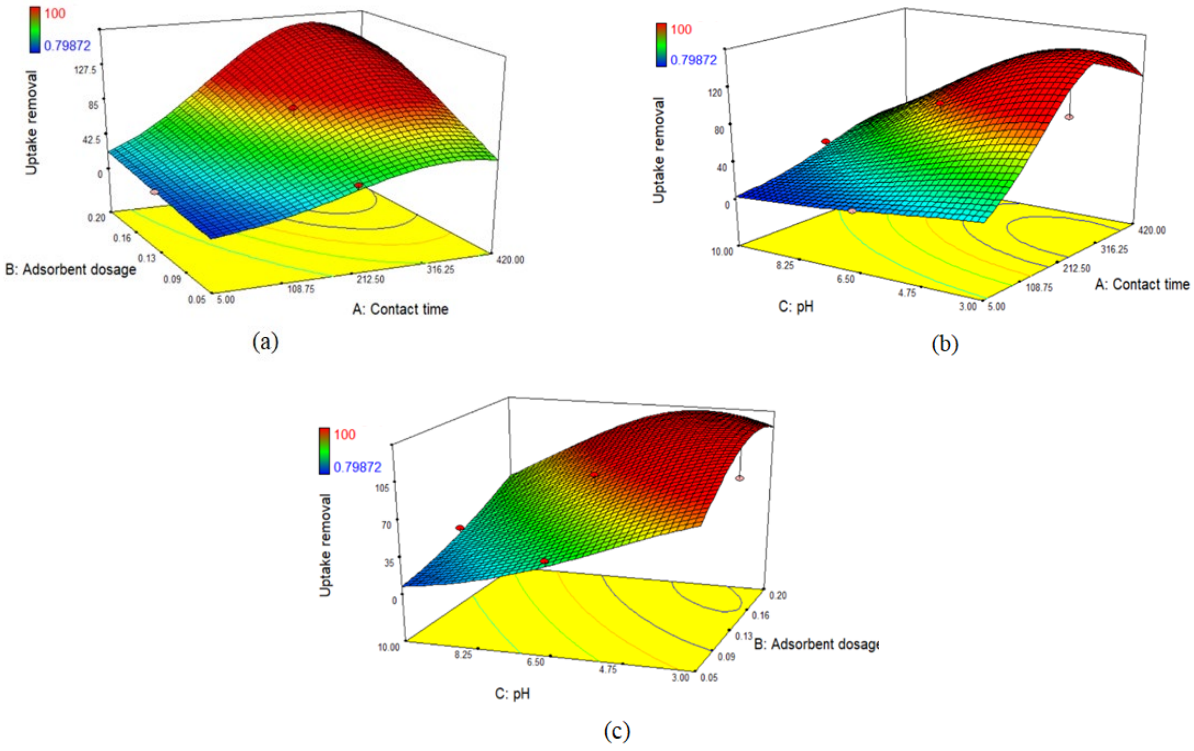


Figure 15: Response surface plots of the interaction effects between (a) contact time and adsorbent dosage, (b) contact time and pH, and (c) adsorbent dosage and pH on uptake removal of RB5

Table 7
RSM experimental conditions for RB5 removal using KH-CH-ECH composite beads, including the corresponding experimental and predicted uptake values

Experimental run	Factors			Experimental % uptake	Predicted % uptake
	Contact time (min)	Adsorbent dosage (g)	pH		
1	5	0.050	3	15.13	16.40
2	5	0.200	3	36.53	35.03
3	5	0.125	6.5	12.85	13.25
4	5	0.050	10	0.80	0.79
5	5	0.200	10	6.57	7.24
6	212.5	0.050	6.5	43.96	38.93
7	212.5	0.125	3	100.00	99.90
8	212.5	0.125	6.5	94.60	85.95
9	212.5	0.125	10	30.94	26.47
10	212.5	0.200	6.5	100.00	92.64
11	420	0.050	3	100.00	98.21
12	420	0.200	3	100.00	99.98
13	420	0.125	6.5	100.00	100.00
14	420	0.050	10	13.10	15.58
15	420	0.200	10	96.34	94.08

This finding indicated that pH exerted a strong influence on the adsorption process, as evidenced in the *p* value reported for pH was <0.0001, which was lesser than adsorbent dosage of having *p* value of 0.0002. Thus, in this study, acidic to nearly neutral conditions were necessary to achieve maximum RB5 removal.

Verification of RSM model

The model equation was validated through the desirability function under optimized conditions provided by the software. As presented in Table 7, a strong agreement was observed between predicted and experimental uptake values of RB5, with deviations not exceeding 9%, thereby demonstrating the robustness of the model and its ability to accurately represent the adsorption behaviour in this study.

CONCLUSION

The present study demonstrated the effectiveness of KH-CH-ECH composite beads for the removal of RB5 from aqueous solutions. Batch adsorption experiments revealed that the adsorption performance was influenced by several factors, including contact time, initial RB5 concentration, adsorbent dosage, agitation rate and solution pH. The equilibrium data were best described by the Freundlich isotherm model (R^2 = 0.9992), suggesting adsorption of RB5 on a heterogeneous surface with non-uniform adsorption sites. KH-CH-ECH composite beads were able to achieve a maximum adsorption capacity of 33.8983 mg/g, indicating its good affinity towards RB5 dye molecules. In addition, kinetic studies revealed that the adsorption process followed pseudo-second order kinetics model, as evidenced by R^2 values approaching unity across all the concentrations. PB identified contact time, adsorbent dosage and pH as the significant factors that affected the adsorption of RB5. These factors were subsequently optimized using RSM and complete dye removal (100%) was achieved under the optimum conditions (212.5 minutes, 0.125 g of KH-CH-ECH composite beads, pH 3). The close agreement between the experimental and predicted results further confirmed the reliability of the developed model. Overall, these findings provided valuable insights into the application of agricultural waste-derived adsorbents for wastewater treatment and supported the potential use of KH-CH-ECH composite beads in sustainable dye removal processes.

ACKNOWLEDGMENTS: This research work received financial support and research facilities assistance from Universiti Tunku Abdul Rahman.

REFERENCES

[1] S. Pourrahim, A. Salem, S. Salem and R. Tavangar, *Environ. Pollut.*, **256**, 113454 (2020), https://doi.org/10.1016/j.envpol.2019.113454

[2] A. B. Mahdi, A. M. Aljeboree and A. F. Alkaim, *J. Chem. Health Risks*, **11**, 203 (2021), https://doi.org/10.22034/jchr.2021.682032
[3] G. Kavitha, M. Govindhan and S. Premkumar, *J. Water Process Eng.*, **80**, 109071 (2025), https://doi.org/10.1016/j.jwpe.2025.109071
[4] H. Alzain, V. Kalimugogo, K. Hussein and M. Karkadan, *Int. J. Res. Rev.*, **10**, 673 (2023), https://doi.org/10.52403/ijrr.20230682
[5] T. Shindhal, P. Rakholiya, S. Varjani, A. Pandey, H. H. Ngo *et al.*, *Bioengineered*, **12**, 70 (2021), https://doi.org/10.1080/21655979.2020.1863034
[6] O. O. Soyinka, I. O. Evbuomwan, T. O. Abodunrin and J. A. Adekoya, *Results Chem.*, **22**, 103130 (2026), https://doi.org/10.1016/j.rechem.2026.103130
[7] B. Lellis, C. Z. Fávaro-Polonio, J. A. Pamphile and J. C. Polonio, *Biotechnol. Res. Innov.*, **3**, 275 (2019), https://doi.org/10.1016/j.biori.2019.09.001
[8] M. R. J. Sarvestani and Z. Doroudi, *J. Water Environ. Nanotechnol.*, **5**, 180 (2020), https://doi.org/10.22090/jwent.2020.02.008
[9] M. K. A. Elnabi, M. A. Ghazy, S. S. Ali, M. Eltarahony and A. Nassrallah, *Microb Cell Fact.*, **24**, 154 (2025), https://doi.org/10.1186/s12934-025-02768-z
[10] V. S. Munagapati, J. C. Wen, C. L. Pan, Y. Gutha, J. H. Wen *et al.*, *Int. J. Phytoremediat.*, **22**, 267 (2019), https://doi.org/10.1080/15226514.2019.1658709
[11] M. Chang and Y. Shih, *J. Environ. Manage.*, **224**, 235 (2018), https://doi.org/10.1016/j.jenvman.2018.07.021
[12] H. Deng, M. Zhang, Y. Cao and Y. Lin, *Environ. Prog. Sustain. Energ.*, **38**, s1 (2018), https://doi.org/10.1002/ep.12976
[13] A. C. Sadiq, A. Olasupo, W. S. Wan Ngah, N. Y. Rahim and F. B. M. Suah, *Int. J. Biol. Macromol.*, **191**, 1151 (2021), https://doi.org/10.1016/j.ijbiomac.2021.09.179
[14] R. Agarwala and L. Mulky, *ChemBioEng Rev.*, **10**, 326 (2023), https://doi.org/10.1002/cben.202200011
[15] Z. Liu, X. Huang, Y. Miao, B. Gao, Y. Shi *et al.*, *Ind. Crop. Prod.*, **187**, 115510 (2022), https://doi.org/10.1016/j.indcrop.2022.115510
[16] M. Bansal, P. K. Patnala and T. Dugmore, *Curr. Res. Green Sustain. Chem.*, **3**, 100036 (2020), https://doi.org/10.1016/j.crgsc.2020.100036
[17] J. O. Quansah, T. Hlaing, F. N. Lyonga, P. P. Kyi, S. H. Hong *et al.*, *Appl. Sci.*, **10**, 3437 (2020), https://doi.org/10.3390/app10103437
[18] A. Hamzezadeh, Y. Rashtbari, S. Afshin, M. Morovati and M. Vosoughi, *Int. J. Environ. Anal. Chem.*, **102**, 254 (2022), https://doi.org/10.1080/03067319.2020.1720011
[19] J. N. Wekoye, W. C. Wanyonyi, P. T. Wangila and M. K. Tonui, *Environ. Chem. Ecotoxicol.*, **2**, 24 (2020), https://doi.org/10.1016/j.enceco.2020.01.004
[20] E. W. C. Chan, S. W. Yeong, C. W. Wong, O. Y. M. Soo, A. C. Y. Phua *et al.*, *J. Appl. Biol. Biotech.*, **11**, 1 (2023), https://doi.org/10.7324/JABB.2023.110101
[21] K. C. Vasconcelos, S. G. Alencar, A. B. Ferro, L. F. A. M. Oliveira, E. J. S. Fonseca *et al.*, *Sep. Purif. Technol.*, **326**, 124787 (2023), https://doi.org/10.1016/j.seppur.2023.124787
[22] R. Zein, H. Fathony, P. Ramadhani and D. Deswati, *J. Serb. Chem. Soc.*, **89**, 123 (2024), https://doi.org/10.2298/JSC230303084Z
[23] R. Ahmad and K. Ansari, *Process Biochem.*, **108**, 90 (2021), https://doi.org/10.1016/j.procbio.2021.05.013
[24] A. H. Jawad, N. S. A. Mubarak and S. Sabar, *Desalin. Water Treat.*, **164**, 378 (2019), https://doi.org/10.5004/dwt.2019.24438
[25] U. B. L. Utami, U. Irawati, Abdulah and M. S. Alim, *J. Ecol. Eng.*, **27**, 213 (2026), https://doi.org/10.12911/22998993/216711
[26] N. Asim, M. H. Amin, M. A. Alghoul, S. A. A. Sulaiman, H. Razali *et al.*, *J. Nat. Fibers.*, **18**, 968 (2019), https://doi.org/10.1080/15440478.2019.1675214
[27] S. Kumar and J. Koh, *Int. J. Mol. Sci.*, **13**, 6102 (2012), https://doi.org/10.3390/ijms13056102
[28] B. A. Al-Mur and M. T. Jamal, *Polymers*, **18**, 546 (2026), https://doi.org/10.3390/polym18050546
[29] M. Poletto, A. J. Zattera, M. M. C. Forte and R. M. C. Santana, *Bioresour. Technol.*, **109**, 148 (2012), https://doi.org/10.1016/j.biortech.2011.11.122
[30] C. Branca, G. D'Angelo, C. Crupi, K. Khouzami, S. Rifici *et al.*, *Polymer*, **99**, 614 (2016), https://doi.org/10.1016/j.polymer.2016.07.086
[31] S. Pokhrel, M. Shrestha, M. Slouf, J. Sirc and R. Adhikari, *Int. J. Compos. Mater.*, **10**, 29 (2020), https://doi.org/10.5923/j.cmaterials.20201002.01
[32] V. S. Munagapati and D. S. Kim, *J. Mol. Liq.*, 220, **540** (2016), https://doi.org/10.1016/j.molliq.2016.04.119
[33] A. El-araby, L. E. Ghadraoui and F. Errachidi, *Molecules*, **27**, 8285 (2022), https://doi.org/10.3390/molecules27238285
[34] M. Batista, M. L. Pinto, F. Antunes, J. Pires and S. Carvalho, *Materials*, **14**, 6701 (2021), https://doi.org/10.3390/ma14216701
[35] J. Shi and J. Li, *Bioresources*, **7**, 3463 (2012), https://doi.org/10.15376/biores.7.3.3463-3475
[36] T. F. S. Evangelista, G. R. S. Andrade, K. N. S. Nascimento, S. B. dos Santos, M. de Fátima Costa Santos *et al.*, *Carbohyd. Polym.*, **245**, 116592 (2020), https://doi.org/10.1016/j.carbpol.2020.116592
[37] J. Zhuang, M. Li, Y. Pu, A. J. Ragauskas and C. G. Yoo, *Appl. Sci.*, **10**, 4345 (2020), https://doi.org/10.3390/app10124345
[38] G. Capobianco, M. L. Antenozio, G. Bonifazi, P. Brunetti, M. Cardarelli *et al.*, *Water*, **15**, 1333 (2023), https://doi.org/10.3390/w15071333
[39] A. Rafiee, N. Mozafari, N. Fekri, M. Memarpour and A. Azadi, *Heliyon*, **10**, e24217 (2024), https://doi.org/10.1016/j.heliyon.2024.e24217

[40] P. Madaninasab, S. Labbaf and H. Salehi, *Macromol. Mater. Eng.*, **311**, e00452 (2026), https://doi.org/10.1002/mame.2025004521of25
[41] D. L. Sills and J. M. Gossett, *Biotechnol. Bioeng.*, **109**, 353 (2012), https://doi.org/10.1002/bit.23314
[42] W. M. F. M. Roslan and M. I. Idris, *RPMME*, **4**, 261 (2023), https://doi.org/10.30880/rpmme.2023.04.02.033
[43] X. Song, F. Chen and F. Liu, *BioResources*, **7**, 652 (2011), https://doaj.org/article/d136e1e82e2e401a974df4a1df8007dd
[44] K. S. Salem, N. K. Kasera, Md. A. Rahman, H. Jameel, Y. Habibi *et al*., *Chem. Soc. Rev.*, **52**, 6417 (2023), https://doi.org/10.1039/D2CS00569G
[45] H. Y. Gan, L. E. Leow and S. T. Ong, *Acta Chim. Slov.*, **64,** 144 (2017), https://doi.org/10.17344/acsi.2016.2983
[46] I. Arslan-Alaton, O. Koba-Ucun, N. Turkten, I. N. Sora and M. Bekbolet, *Water*, **15**, 906 (2023), https://doi.org/10.3390/w15050906
[47] K. C. Lai, L. Y. Lee, B. Y. Z. Hiew, T. C. K. Yang, G. T. Pan *et al*., *J. Taiwan Inst. Chem. Eng.*, **114**, 57 (2020), https://doi.org/10.1016/j.jtice.2020.09.024
[48] N. T. H. Hoa, N. T. Quynh, V. D. Nguyen, T. N. Nguyen, B. Q. Huy *et al*., *Water*, **17**, 1678 (2025), https://doi.org/10.3390/w17111678
[49] A. F. Al-Mahmodi, M. R. Atta, Y. Munusamy and B. N. S. Al-Dhawi, *Chem. Thermodyn. Therm. Anal.*, **18**, 100174 (2025), https://doi.org/10.1016/j.ctta.2025.100174
[50] B. An, *Processes*, **8**, 1194 (2020), https://doi.org/10.3390/pr8091194
[51] P. Samiyammal, A. Kokila, L. A. Pragasan, R. Rajagopal, R. Sathya *et al*., *Environ. Res.*, **212**, 113497 (2022), https://doi.org/10.1016/j.envres.2022.113497
[52] M. Bellaj, K. Aziz, M. E. Achaby, M. E. Haddad, L. Gebrati *et al*., *Chem. Eng. Sci.*, **285**, 119615 (2024), https://doi.org/10.1016/j.ces.2023.119615
[53] W. Y. Chung and S. T. Ong, *J. Phys. Sci.*, **32**, 91 (2021), https://doi.org/10.21315/jps2021.32.1.7
[54] Y. Cheng, A. Li, W. Shi and L. Zhao, *Chem. Eng. J.*, **481**, 148535 (2024), https://doi.org/10.1016/j.cej.2024.148535
[55] G. K. Latinwo, A. O. Alade, S. E. Agarry and E. O. Dada, *Polycycl. Aromat. Comp.*, **41**, 400 (2019), https://doi.org/10.1080/10406638.2019.1591467
[56] A. Magdy, M. R. Mostafa, S. A. Moustafa, G. G. Mohamed and O. A. Fouad, *Sci. Rep.*, **14**, 24392 (2024), https://doi.org/10.1038/s41598-024-73697-x
[57] M. R. Islam and M. G. Mostafa, *Sustain. Water Resour. Manag.*, **8**, 52 (2022), https://doi.org/10.1007/s40899-022-00640-1
[58] A. Kheddo, L. Rhyman, M. I. Elzagheid, P. Jeetah and P. Ramasami, *SN Appl. Sci.*, **2**, 2170 (2020), https://doi.org/10.1007/s42452-020-03922-5
[59] E. Bazrafshan, F. K. Mostafapour, S. Rahdar and A. H. Mahvi, *Desalin. Water Treat.*, **54**, 2241 (2015), https://doi.org/10.1080/19443994.2014.895778
[60] N. Mengelizadeh and H. Pourzamani, *Health Scope*, **9**, 102443 (2020), https://doi.org/10.5812/jhealthscope.102443
[61] V. S. Munagapati, V. Yarramuthi, Y. Kim, K. M. Lee and D. S. Kim, *Ecotoxicol. Environ. Saf.*, **148**, 601 (2018), https://doi.org/10.1016/j.ecoenv.2017.10.075
[62] V. S. Munagapati, J. C. Wen, C. L. Pan, Y. Gutha and J. H. Wen, *J. Mol. Liq.*, **285**, 375 (2019), https://doi.org/10.1016/j.molliq.2019.04.081
[63] I. Langmuir, *J. Am. Chem. Soc.*, **40**, 1361 (1918)
[64] A. K. Topaloğlu and Y. Yildirim, *Membr. Water Treat.*, **12**, 23 (2021), https://doi.org/10.12989/mwt.2021.12.1.023
[65] T. C. Silva, T. J. M. Fraga, M. Carvalho, V. L. Silva and M. A. Da Motta, *Lat. Am. Appl. Res.*, **48**, 101 (2018), https://doi.org/10.52292/j.laar.2018.266
[66] A. N. R. Leal, A. C. A. Lima, M. G. F. A. Azevedo, D. K. D. N. Santos, L. E. M. C. Zaidan *et al*., *Sci. Plen.*, **17**, 034201 (2021), https://doi.org/10.14808/sci.plena.2021.034201
[67] H. M. F. Freundlich, *J. Phys. Chem.*, **57**, 385 (1906)
[68] S. Brunauer, P. H. Emmett and E. Teller, *J. Am. Chem. Soc.*, **60**, 309 (1938)
[69] S. Lagergren, *Kungl. Svenska Vetenskapsakad. Handl.*, **24**, 1 (1898)
[70] Y. S. Ho and G. McKay, *Process Biochem.*, **34**, 451 (1999), https://doi.org/10.1016/S0032-9592(98)001125
[71] J. K. Chong and S. T. Ong, *Stud. Univ. Babes-Bolyai Chem.*, **66**, 171 (2021), https://doi.org/10.24193/subbchem.2021.4.13
[72] Z. Hussain, N. Chang, J. Sun, S. Xiang, T. Ayaz *et al*., *Hazard. Mater.*, **422**, 126778 (2022), https://doi.org/10.1016/j.jhazmat.2021.126778
[73] M. N. Roy, Md. T. Hossain, Md. Z. Hasan, K. Islam, Md. Rokonuzzaman *et al*., *Text. Leather Rev.*, **6**, 211 (2023), https://doi.org/10.31881/tlr.2023.030
[74] J. Y. Tong, S. T. Ong and S. T. Ha, *Cellulose Chem. Technol.*, **59**, 1213 (2025), https://doi.org/10.35812/CelluloseChemTechnol.2025.59.100